

(revised, 12/20/05)

## **Speed of Light and Laser Studies**

Advanced Laboratory, Physics 407  
University of Wisconsin  
Madison, WI 53706

### ***Abstract***

The speed of light is determined from a time of flight measurement of a short pulse of light. The pulse of light is generated by a dye laser and sent over both a long and a short path and detected by a photomultiplier tube. The velocity of light is then determined from measurements of the light path lengths and the time delay between signals. For the second part, the fluorescence spectrum of three dyes is measured as a function of wavelength using a photodiode detector.

## ***METHOD***

This experiment consists of two parts.

1. The short pulse of light emitted from a dye laser is split into two beams. One beam is sent directly to the input of a photomultiplier tube, while the other beam propagates along a much longer path consisting of several mirrors located at the end of the room before being detected by the photomultiplier tube. The speed of light is measured from the time delay between two pulses of light.
- 3 The fluorescence spectra of three dyes used in the dye lasers are measured using a photodiode and the grating monochromator built into the dye laser.

The measurement details are described in the following text. There are three Appendices containing apparatus details. A: Dye Lasers, B: Photomultiplier Tubes, and C: Photodiode Detectors.

## ***EQUIPMENT***

1. Nitrogen pumped Dye laser with 3 dyes.
2. Photomultiplier tube with power supply.
3. Digital Oscilloscope (300 MHz).
4. Assorted plates of glass.
5. 3 adjustable mirrors.
6. Photodiode and power supply.

## ***MANUALS***

1. VSL-337 Nitrogen Laser and Dye laser Modules, Laser Science, Inc.
2. Photodiode detector manual.

## Part 1: Speed of light

To measure the speed of light, the time required for a pulse of light to travel a distance will be measured. To produce a high intensity and sufficiently short pulse of light for this measurement a nitrogen pumped dye laser is used. Before starting, you should look up the speed of light and the index of refraction for air, and read the operation manual for the laser.

Step 1. Familiarize yourself with the operating principles of a nitrogen-pumped dye laser. Insert the quartz cuvette containing Rhodamine 6G being careful not to touch the surface of the cuvette, and adjust the monochromator setting to 590. Observe the light pulse on a note card or other surface. Adjust the monochromator and note that the light quality observed when lasing is different from the fluorescence, which is seen even when the monochromator is not set to the laser wavelength.

Step 2. Familiarize yourself the operating principles of a photomultiplier tube. Turn on the PM tube high voltage (start at 400 volts) and measure the detected current on an oscilloscope with the room lights both on and off.

Step 3. Using a fast digital oscilloscope, measure the light pulse from the dye laser by reflecting a small part of the laser light into the PM tube. This is accomplished using one of the plates of glass provided. To trigger the oscilloscope, use both the internal trigger on the signal itself and the external trigger by triggering both the laser and the oscilloscope with a function generator. The noise generated by the switching of the high voltage onto the nitrogen lasers provides a sufficient signal from the PM tube for triggering. How wide is the laser pulse?

Step 4. Set up the long path length by using reflections from the three mirrors (down-back-down-back). Direct the final beam onto the PM tube so that both the initial pulse and the second pulse are seen simultaneously on the oscilloscope. If using a digital oscilloscope with pulse

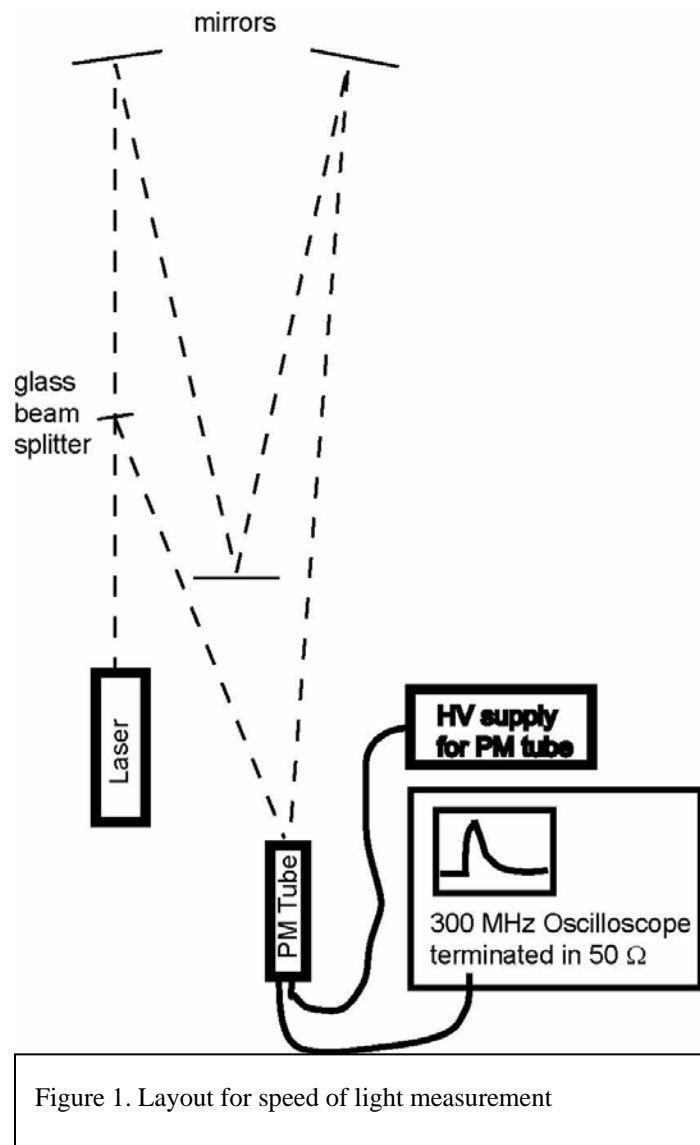


Figure 1. Layout for speed of light measurement

averaging, the signal quantity can be greatly improved by summing over multiple pulses. Measure the time separation between the two pulses. How accurate is this measurement? What is the major source of uncertainty in your measurement of the time separation?

Step 5. Carefully measure the optical path lengths in the experiment using a plumb bob and a tape measure. Determine the difference in pathlengths for the two laser pulses. What are the major sources of uncertainty in the pathlength measurements? Is this uncertainty more or less important than the time difference uncertainty in step 4?

Step 6. Calculate the speed of light in air. Estimate the uncertainty estimate of your measurement. How does it compare with the predicted value?

## Part 2: Florescence of Dyes

The dyes used in the dye laser have the interesting quality that once excited they floresce (emit light over a broadband continuum (typically ~10 Angstroms). A nitrogen laser is used to pump the dyes into excited states. By choosing a dye that floresces at a chosen color, lasing can be achieved by placing the excited dye in a resonant cavity. This makes it possible to create a laser at virtually any frequency by choosing an appropriate dye. Here monitoring the laser power with a photodiode and scanning the resonant wavelength of the cavity measures the gain curves of three dyes.

Step 1. Read the manual on the photodiode detector. Note that the sensitivity of the photodiode varies with wavelength (the calibration curve is given in the photodiode appendix to this writeup). The calibration curve will be used to correct the measurements and estimate the actual gain in the following steps.

Step 2. Turn on the laser with your first dye. Use the plate glass to partially reflect the laser beam into the photodiode detector, and observe the signal directly on the oscilloscope. Be careful not to saturate the photodiode with light (as seen by a “clipped” signal). What determines the pulse-width of the detected signal?

Step 3. Vary the monochrometer setting and record the signal level from the photodiode using the oscilloscope. Correct your data for the sensitivity of the photodiode and plot the signal level vs. wavelength.

Step 4. Repeat Step 3 for the other two dyes. Plot all three curves on one graph.

## APPENDIX A: Dye Laser

Gas lasers and solid state lasers can easily be designed for a single frequency oscillation; the output frequency may be tuned continuously over the band-width of the Doppler-broadened gain curve. Unfortunately this tuning range is relatively narrow and the application of these gas lasers to atomic and molecular spectroscopy is somewhat restricted to studies of the laser transitions themselves, or to accidental coincidences with molecular absorption lines. It would therefore seem that the new and powerful technique of saturated absorption spectroscopy was also of relatively limited applicability. Dye lasers take advantage of the broadband fluorescence of dyes resulting from many close energy levels for molecular transitions to provide tunability over a band of frequencies.

### *Tunable organic dye lasers*

Many organic compounds that absorb strongly in certain regions of the visible spectrum also fluoresce very efficiently, emitting radiation which covers a large wavelength range. The first descriptions of stimulated emission from these fluorescent organic dyes in liquid solution were reported almost simultaneously by Sorokin and Lankard (1966) and Schafer et al. (1966). It was not long before Soffer and McFarland (1967) had demonstrated that the stimulated emission was also tunable and the rapid development of tunable dye lasers had commenced.

The energy-level scheme of a typical organic dye molecule in dilute solution is shown schematically in Figure 2. It consists of a ground state  $S_0$  and a series of excited singlet levels  $S_1, S_2, \dots$  together with another series of triplet levels  $T_1, T_2, \dots$  in which the lowest level lies about  $15,000 \text{ cm}^{-1}$  above the ground state  $S_0$ . The energy level separation  $S_0 - S_1$  is typically about  $20,000 \text{ cm}^{-1}$ . In the singlet states the spin of the active electron and that of the remainder of the molecule are antiparallel, while in the triplet states the spins are parallel. Transitions between states of the same multiplicity give rise to the intense absorption and fluorescence spectra of the dye while singlet-triplet radiative transitions involve a spin flip and are therefore far less probable. Each electronic level is also associated with an array of vibrational and rotational levels. The vibrational levels are spaced by intervals of  $1400\text{-}1700 \text{ cm}^{-1}$  while the spacing of the rotational levels is smaller by a factor of approximately 100 (consequently this is too small to be shown in Figure 2). Due to rapid relaxation process the rotational and vibrational levels are smeared out to form broad continuous energy bands. These account for the continuous absorption and emission spectra, examples of which are shown in Figure 3 for the case of the well-known laser dye rhodamine 6G in ethyl

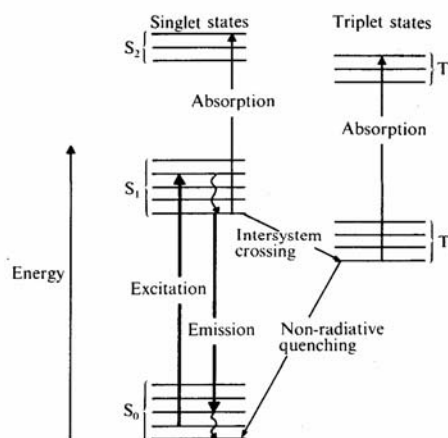


Figure 2. Schematic Energy Level Diagram of a Typical Dye Molecule.

alcohol solution. The colour of the dye is determined by the broad absorption band  $S_0$  to  $S_1$  which results from the excitation of an electron in a  $\pi$  orbital.

When the dye solution is illuminated by light whose wavelength falls in the absorption band, molecules are optically excited from the level  $S_0$  into some rotational-vibrational level belonging to the excited singlet state,  $S_1$ . Following the excitation, rapid collisions with other molecules dissipate the excess vibrational-rotational energy and the molecule relaxes to the lowest vibrational level of the  $S_1$  state in a time of the order of  $10^{-11}$ – $10^{-12}$  s. From here the molecule can decay by spontaneous emission, with a radiative lifetime  $\tau_s \approx 10^{-9}$  s to any of the rotational-vibrational levels of the ground state. Consequently the emitted light is of longer wavelength than the pumping radiation. Finally non-radiative relaxation processes return the molecule to the  $v=0$  level of the electronic ground state,  $S_0$ .

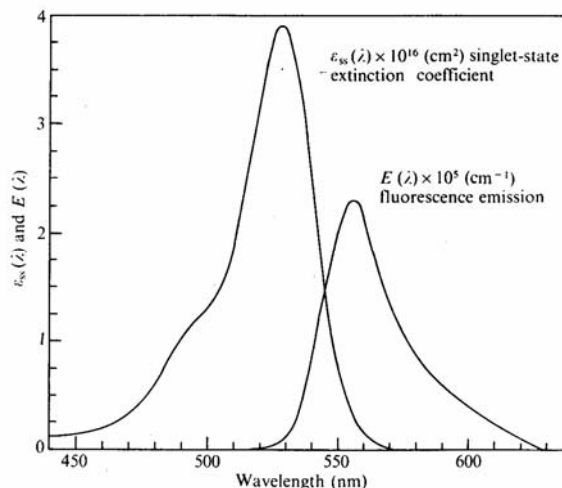


Figure 3. Absorption and Fluorescence Spectra of the Laser Dye Rhodamine 6G.

If the intensity of the pumping radiation is very high, exceeding about  $100 \text{ kW cm}^{-2}$ , a population inversion between  $S_1$  and  $S_0$  may be attained. Light amplification by the stimulated emission of radiation is then possible over almost the entire fluorescence band with the exception of that part which is effectively overlapped by the absorption band of the molecule. In the absence of frequency-selective feedback, the dye laser will oscillate on a band approximately 10-50 Å wide close to the peak of the fluorescence curve. However, due to the rapid thermalization of the vibrational and rotational levels, the spectral profile of the gain curve is essentially homogeneously broadened and it is possible to channel almost the entire available energy into a narrow spectral range by using a laser cavity with wavelength-selective feedback. Thus continuously tunable dye laser oscillation may be obtained.

**Molecular nitrogen laser-pumped dye lasers.** A particularly reliable and convenient pump source is the pulsed nitrogen laser operating at 337.1 nm. The short wavelength of this laser radiation excites many dyes to high-lying singlet levels, but in all cases the molecules relax very quickly to the bottom edge of the lowest excited singlet level, dissipating the excess energy in the solvent, and dye laser oscillation occurs on the  $S_1 \rightarrow S_0$  transition. Since most dyes have a strong absorption band in the ultraviolet region the nitrogen laser provides an almost universal pump source. The short pulse length and high repetition frequency of this laser provide a convenience similar to that of C.W. operation and it is one of the most widely used systems in

atomic spectroscopy.

A schematic diagram of the nitrogen laser-pumped dye laser system is shown in Figure 4. The nitrogen laser consists of a rectangular channel 1 m long through which a rapid discharge is passed from a triggered high-voltage capacitor system. Nitrogen molecules are excited to the  $C^3\Pi_u$  state by collisions with fast electrons and a transient inversion is created on the  $B^3\Pi_g \leftrightarrow C^3\Pi_u$  ultraviolet violet emission band. The radiation emitted by the laser is self-terminating because the lower level has a longer lifetime than that of the upper level and in most of these devices the output consists of a pulse of amplified spontaneous emission at 337.1 nm lasting 7-10 ns and having a peak power of 300kW.

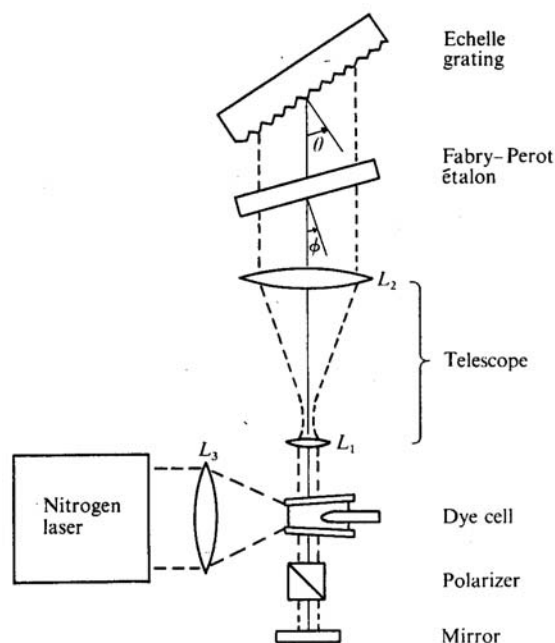


Figure 4 Dye Laser with Narrow Bandwidth Output Pumped by Pulsed Nitrogen Laser.

The radiation from the nitrogen laser emerges in the form of a beam of rectangular cross-section, approximately 5 mm x 40 mm, which is focussed by a spherical quartz lens into a line near the inner wall of the dye cell. The active volume of the dye forms a cylindrical filament about 0.2 mm diameter and 10 mm long having a single pass gain which approaches  $10^3 \text{mm}^{-1}$  under these conditions. The optical cavity of the dye laser is about 40 cm long and consists of a plane dielectrically-coated mirror at one end and a Littrow mounted diffraction grating at the other.

In order to achieve a narrow bandwidth tunable output one mirror of the normal laser cavity is usually replaced by a diffraction grating as shown in Figure 4. The grating normal makes an angle theta with the axis of the cavity and in this Littrow arrangement the condition

$$2d \sin\theta = m\lambda \quad m = 1, 2, \dots$$

must be satisfied for radiation to be reflected back along the cavity axis. In this equation  $\lambda$  is the oscillating wavelength of the laser and  $d$  is the grating spacing. Light of other wavelengths is not reflected back along the cavity axis and consequently this radiation sees a very lossy resonator and oscillation is prevented. Thus narrow bandwidth laser output is obtained and wavelength tuning may be accomplished simply by rotating the grating. Prisms, Fabry-Perot etalons, and combinations of these elements with diffraction gratings have all been used as tuning elements in dye lasers and the bandwidths obtained range typically from 0.3-3.0 Å.

### **Specifications for Physics 407 Dye Laser**

<b>Nitrogen laser:</b>	<b>VSL-337</b>
Maximum output power:	2 mW
Peak output power:	40 kW
Pulse length:	3 ns
Pulse energy:	120 $\mu$ J
Pulse repetition rate:	1-20 pulses per second
Plasma cartridge lifetime:	20 million pulses

### **Tunable Dye Laser Module**

Three dyes are provided for the experiment. Each dye is in a quartz cuvette that can be inserted into the dye laser cavity. Be careful not to touch the sides of the cuvette with your fingers. The positive feedback required for lasing is provided by a grating monochromator which is tuned to the desired wavelength. The dyes are made by mixing powder with ethanol or methanol solvent to 0.005 mole/liter.

<u>Color</u>	<u><math>\lambda</math></u>	<u>Dye</u>	<u>Molecular Weight</u>
Yellow	590 nm	Rhodemine 6G	479
Green	540 nm	Fluorescein Disodium Salt	412.31
Blue	460 nm	TD4MC	231

## APPENDIX B: Photomultiplier Tubes

Photomultipliers (PM's) are electron tube devices that convert light into a measurable electric current. They are extremely sensitive and, in nuclear and high-energy physics, are most often associated with scintillation detectors, although their uses are quite varied. It is nevertheless in this context that we will discuss the basic design and properties of photomultipliers, their characteristics under operation and some special techniques.

### Basic Construction and Operation

Figure 5 shows a schematic diagram of a typical photomultiplier. It consists of a cathode made of photosensitive material followed by an electron collection system, an electron multiplier section (or dynode string as it is usually called) and finally an anode from which the final signal can be taken. All parts are usually housed in an evacuated glass tube so that the whole photomultiplier has the appearance of an old-fashion electron tube.

During operation a high voltage is applied to the cathode, dynodes and anode such that a potential "ladder" is set up along the length of the cathode - dynode - anode structure. When an incident photon impinges upon the photocathode, an electron is emitted via the photoelectric effect. Because of the applied voltage, the electron is then directed and accelerated toward the first dynode, where upon striking, it transfers some of its energy to the electrons in the dynode. This causes secondary electrons to be emitted, which in turn, are accelerated towards the next dynode where more electrons are released and further accelerated. An electron cascade down the dynode string is thus created. At the anode, this cascade is collected to give a current which can be amplified and analyzed.

Photomultipliers may be operated in continuous mode, i.e., under a constant illumination, or in pulsed mode for observing single photons. In either mode, if the cathode and dynode systems are assumed to be linear, the current at the output of the PM will be directly proportional to the number of incident photons.

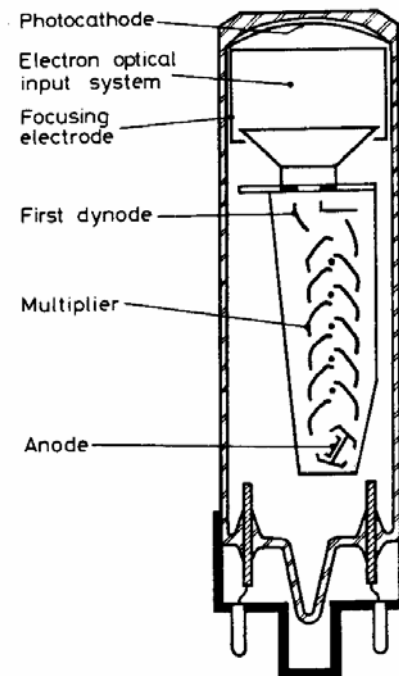


Figure 5. PM tube cross section.

### Photocathode and efficiency

As we have seen, the photocathode converts incident light into a current of electrons by the photoelectric effect. To facilitate the passage of this light, the photosensitive material is

deposited in a thin layer on the inside of the PM window which is usually made of glass or quartz. From Einstein's well-known formula,

$$E=hf-W,$$

where  $E$  is the kinetic energy of emitted electron,  $f$  is the frequency of incident light and  $W$  is the work function, it is clear that a certain minimum frequency is required before the photoelectric effect may take place. Above this threshold, however, the probability for this effect is far from being unity. Indeed, the efficiency for photoelectric conversion varies strongly with the frequency of the incident light and the structure of the material. This overall spectral response is expressed by the *quantum efficiency*,  $\eta$ ,

$$\eta(\lambda) \equiv \frac{\text{number of photoelectrons released}}{\text{number of incident photons on cathode}}$$

where  $\lambda$  is the wavelength of the incident light.

Most of the photocathodes employed today are made of semiconductor materials formed from antimony plus one or more alkali metals. The choice of semiconductors rather than metals or other photoelectric substances lies in their much greater quantum efficiency for converting a photon to a *usable* electron. Indeed, in most metals, the quantum efficiency is not greater than 0.1% which means that an average of 1000 photons is needed to release one photoelectron. In contrast semiconductors have quantum efficiencies of the order of 10 to 30%, some two orders of magnitude higher! This difference is explained by their different intrinsic structures.

Figure 6 shows a graph of quantum efficiency vs  $\lambda$  for some of the more common photoelectric materials used in photomultipliers today. In general, the spectral response of these materials is such that only a certain band of wavelengths is efficiently converted.

When choosing a PM, therefore, the primary consideration should be its sensitivity to the wavelength of the incident light. For the photocathodes shown in Figure 6 the efficiency peaks near  $\approx 400$  nm. More than 50 other types of materials are in use, however, with spectral sensitivities varying from the infra-red to the ultraviolet.

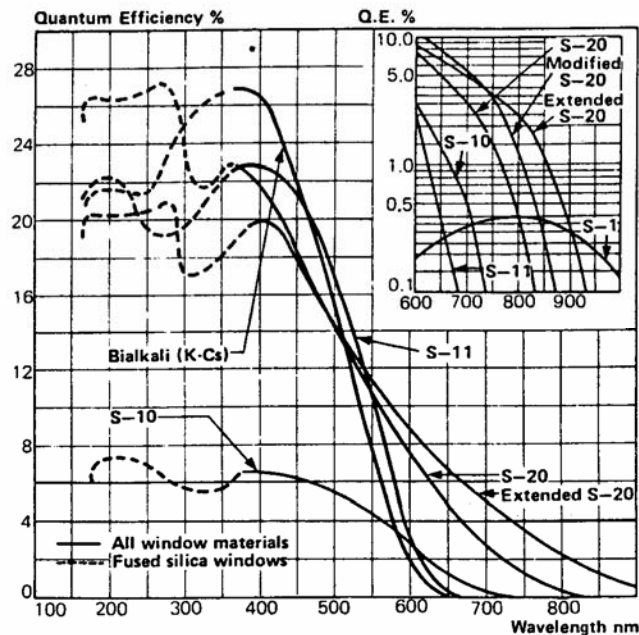


Figure 6 Quantum efficiencies for several PM tube photocathode materials.

## The Electron-Multiplier Section

The electron-multiplier system amplifies the weak primary photocurrent by using a series of secondary emission electrodes or *dynodes* to produce a measurable current at the anode of the photomultiplier. The gain of each electrode is known as the *secondary emission factor*. The theory of secondary electron emission is very similar to that described for photoelectric emission except that the photon is now replaced by an electron. On impact, energy is transferred directly to the electrons in the dynode material allowing a number of secondary electrons to escape. Since the conducting electrons in metals hinder this escape, as we have seen, it is not surprising that insulators and semiconductors are also used here as well.

One difference exists, however, in that an electric field must be maintained between the dynodes to accelerate and guide the electrons along the multiplier. Thus the secondary emission material must be deposited on a conducting material. A common procedure used today is to form an alloy of an alkali or alkaline earth metal with a more noble metal. During the mixing process, only the alkaline metal oxidizes, so that a thin insulating coating is formed on a conducting support. Materials in common use today are Ag - Mg, Cu - Be and Cs - Sb. These have varying advantages but all meet the requirements of a good dynode material:

- 1) high secondary emission factor, i.e., the average number of secondary electrons emitted per primary electron;
- 2) stability of secondary emission effect under high currents;
- 3) low thermionic emission, i.e., low noise.

Most conventional PM's contain 10 to 14 stages, with total overall gains of up to being obtained.

Like the photocathode, use has also been made of negative affinity materials as dynodes, in particular GaP. With this material the individual gain of each dynode is greatly increased so that the number of stages in a PM can be reduced. After emission from the photocathode, the electrons in the PM must be collected and focused onto the first stage of the electron multiplier section. This task is performed by the electron-optical input system. In most PM's, collection and focusing is accomplished through the application of an electric field in a suitable configuration. Magnetic fields or a combination of electric and magnetic fields may also be employed in principle, but their use is extremely rare. Figure 7 gives a schematic diagram of a typical electron-optical input system. Here an accelerating electrode at the same potential as the first dynode of the electron multiplier is used in conjunction with a focusing electrode placed on the side of the glass housing.

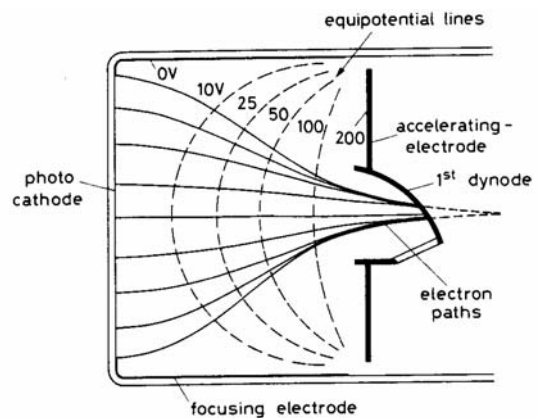
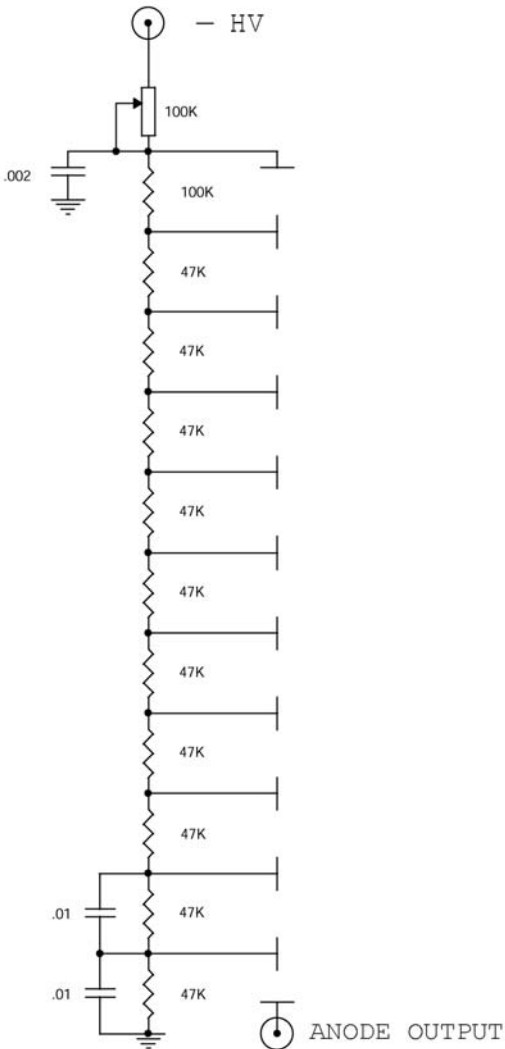


Figure 7. Focusing geometry for photocathode and first dynode. The geometry is optimized to have similar times for flight for electrons emitted from different positions on

# Photomultiplier for Velocity of Light Experiment

Photomultiplier RCA 6199  
 Photocathode Diameter 1.24"  
 Stages 10  
 QE (CsSb S11) 0.1  
 Gain at Max V  $2.8 \times 10^6$  @ 1250V



Bias circuit for PM tube.



**6199**

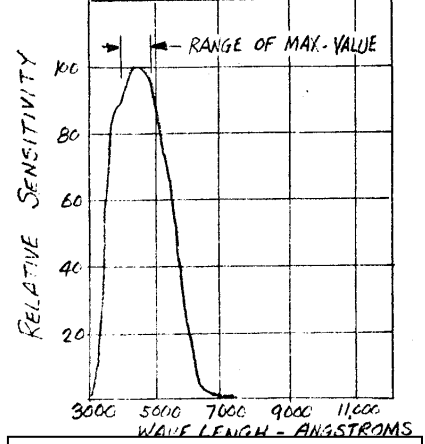
**MULTIPLIER PHOTOTUBE**

10-STAGE, HEAD-ON TYPE WITH  
1.24" SEMITRANSSPARENT CATHODE AND S-11 RESPONSE

DATA	
<b>General:</b>	
Spectral Response . . . . .	S-11
Wavelength of Maximum Response . . . . .	4400 ± 500 angstroms
Cathode, Semitransparent:	
Shape . . . . .	Circular
Window:	
Area . . . . .	1.2 sq. in.
Minimum diameter . . . . .	1.24 in.
Index of refraction . . . . .	1.51
Direct Interelectrode Capacitances (Approx.):	
Anode to dynode No.10 . . . . .	4 μmf
Anode to all other electrodes . . . . .	7 μmf
Maximum Overall Length . . . . .	4-9/16"
Seated Length . . . . .	3-7/8" ± 3/16"
Maximum Diameter . . . . .	1-9/16"
Mounting Position . . . . .	Any
Weight (Approx.) . . . . .	2 oz
Bulb . . . . .	T-12
Base . . . . .	Small-Shell Duodecal 12-Pin (JEDEC No.812-43), Non-hygroscopic 12AE
Basing Designation for BOTTOM VIEW . . . . .	
Pin 1 - Dynode No.1	Pin 7 - Dynode No.10
Pin 2 - Dynode No.3	Pin 8 - Dynode No.8
Pin 3 - Dynode No.5	Pin 9 - Dynode No.6
Pin 4 - Dynode No.7	Pin 10 - Dynode No.4
Pin 5 - Dynode No.9	Pin 11 - Dynode No.2
Pin 6 - Anode	Pin 12 - Cathode
 <p>DIRECTION OF LIGHT: INTO END OF BULB</p>	
<b>Maximum Ratings, Absolute Values:</b>	
ANODE-SUPPLY VOLTAGE (DC or Peak AC) . . . . .	1250 max. volts
SUPPLY VOLTAGE BETWEEN DYNODE No.10 AND ANODE (DC or Peak AC) . . . . .	250 max. volts
DYNODE-No.1 SUPPLY VOLTAGE (DC or Peak AC) . . . . .	300 max. volts
AVERAGE ANODE CURRENT . . . . .	0.75 max. ma
AMBIENT TEMPERATURE . . . . .	75 max. °C
* Averaged over any interval of 30 seconds maximum.	

8-56

DATA 1



S-11 photoresponse

## APPENDIX C: Photodiode Detectors

Semiconductor  $p-n$  junctions are used widely for optical detection. In this role they are referred to as junction photodiodes. The main physical mechanisms involved in junction photodetection are illustrated in Figure 8. At A, an incoming photon is absorbed in the  $p$  side creating a hole and a free electron. If this takes place within a diffusion length (the distance in which an excess minority concentration is reduced to  $e^{-1}$  of its peak value, or in physical terms, the average distance a minority carrier traverses before recombining with a carrier of the opposite type) of the depletion layer, the electron will, with high probability, reach the layer boundary and will drift under the field influence

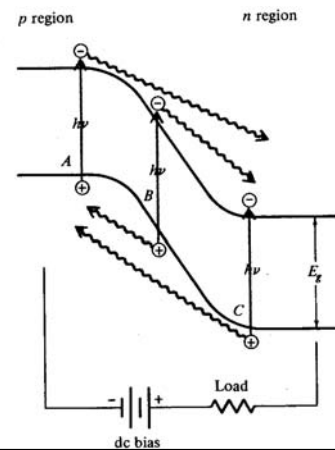


Figure 8 The three types of electron-hole pair creation by absorbed photons that contribute to current flow in a  $p-n$  junction.

across it. An electron traversing the junction contributes a charge  $e$  to the current flow in the external circuit. If the photon is absorbed near the  $n$  side of the depletion layer, as shown at C the resulting hole will diffuse to the junction and then drift across it again, giving rise to a flow of charge  $e$  in the external load. The photon may also be absorbed in the depletion layer as at B, in which case both the hole and electron which are created drift (in opposite directions) under the field until they reach the  $p$  and  $n$  sides, respectively. Since in this case each carrier traverses a distance that is less than the full junction width, the contribution of this process to charge flow in the external circuit is,  $e$ . In practice this last process is the most desirable, since each absorption gives rise to a charge  $e$ , and delayed current response

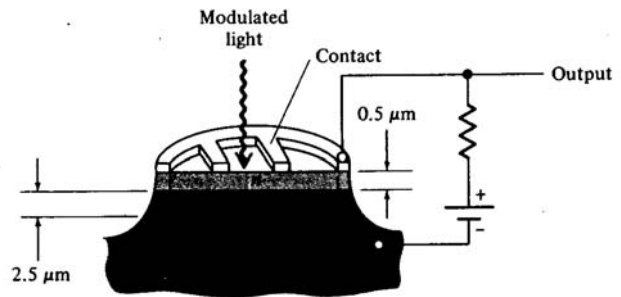


Figure 9. A  $p-i-n$  photodiode.

caused by finite diffusion time is avoided. As a result, photodiodes often use a  $p-i-n$  structure in which an intrinsic high resistivity (i) layer is sandwiched between the  $p$  and  $n$  regions. The potential drop occurs mostly across this layer, which can be made long enough to insure that most of the incident photons are absorbed within it. Typical construction of a  $p-i-n$  photodiode is shown in Figure 9.

It is clear from Figure 9 that a photodiode is capable of detecting only radiation with photon energy  $h\nu > E_g$ , where  $E_g$  is the energy gap of the semi-conductor. If, on the other hand,  $h\nu > E_g$ , the absorption, which in a semiconductor increases strongly with frequency, will take place entirely near the input face (in the  $n$  region of Figure 9) and the minority carriers generated by absorbed photons will recombine with majority carriers before diffusing to the depletion layer. This event does not contribute to the current flow and, as far as the signal is concerned, is wasted. This is why the photo response of diodes drops off when  $h\nu > E_g$ . Typical frequency response curves of photo-diodes are shown in Figure 10. The number of carriers flowing in the external circuit per incident photon, the so-called quantum efficiency, is seen to approach 50% in Ge.

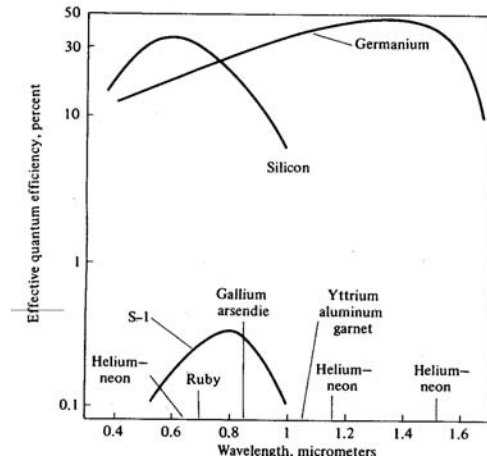


Figure 10. Quantum efficiencies for silicon and germanium photodiodes compared with the efficiency of the S-1 photomultiplier tube.

**Specifications for Physics 407 Photodiode Detector**

The photodiode detector used in the experiment comes mounted in a housing and coupled with a electronics capable of averaging many laser pulses together. In this lab, the electronics are used as a power supply, and the photodiode signal is observed directly on the oscilloscope.

**SILICON PHOTODIODE**

- ACTIVE AREA : 100mm<sup>2</sup>**
- WAVELENGTH RANGE : 330-1150nm**
- RESPONSITIVITY : >.5A/W AT 900nm**

